GEOGRAFICKÝ ČASOPIS / GEOGRAPHICAL JOURNAL 77 (2025) 3, 155-165
DOI: https://doi.org/10.31577/geogrcas.2025.77.3.04

INSTITUTE OF GEOGRAPHY SLOVAK ACADEMY OF SCIENCES

Geografický časopis
Geographical Journal

Modeling future urban expansion and land use transitions in Gorgan Region of Iran using spatial prediction techniques

Mohsen Zabihi[1]*, Ahmadreza Chahardehi[2], Alireza Motevalli[3], Raoof Mostafazadeh[4]

[1] Department of Watershed Management Sciences and Engineering, Faculty of Natural Resources, Tarbiat Modares University, Tehran, Iran, mohsen_zabihi69@yahoo.com
[2] Department of Survey Engineering- Geographic Information Systems, Faculty of Civil Engineering, Lamei Gorgani Institute of Higher Education, Gorgan, Iran, ahmadrezachardehi@protonmail.com
[3] Department of Agroecology, Aarhus University, Tjele, Denmark, arm@agro.au.dk
[4] Department of Natural Resources, Faculty of Agriculture and Natural Resources, University of Mohaghegh Ardabili, Ardabili, Iran, raoofmostafazadeh@uma.ac.ir
* Corresponding author

Abstract

The continuous expansion of urban areas without considering all the influencing factors has led to numerous problems in the field of urbanization. However, urban development modeling serves as a valuable tool for explaining the interrelationships between the man-made and the natural environment. In this context, the current research aims to model the spatial development of human-made areas using Land Change Model (LCM) module and Markov Chain in Gorgan region. For this purpose, LULC maps for the years 1991, 2006, and 2021 were prepared using Landsat images and Support Vector Machine (SVM) model and the trend of changes during the study period was evaluated. Furthermore, potential transition modeling and predictions for the years 2036 and 2051 were performed using Multilayer Perceptron (MLP) and Markov Chain methods, respectively. The results indicate an accuracy of over 75% for the generated LULC maps in the study area. The increasing trend in residential, orchard, and rainfed agricultural LULC classes and the decreasing trend in forest, irrigated agricultural, and rangeland LULC classes during the research period are among the findings of this study. Additionally, urban development intensity during the period from 2006 to 2021 has been greater than the period from 1991 to 2006. The conversion of 1.83 square kilometers of irrigated agricultural land to residential and orchard areas in the Gorgan region area occurred during the time period from 1991 to 2006. In general, the transformation of LULC classes from irrigated agriculture, forest, and rangeland to residential, rainfed agriculture, and orchard classes in Gorgan region predominates. The results and the approach used in this research highlight the efficiency of satellite data and information in the preparation and monitoring of LULC changes and its application in urban development management.

Key words:
LULC planning, Markov chain, satellite image classification, environmental protection

1 INTRODUCTION

The continuous growth in population and its associated consequences, including urbanization, industrialization, agricultural expansion, and LULC changes, have consistently demonstrated adverse impacts on ecosystems. These effects encompass occurrences such as floods, soil erosion, decreased biodiversity, soil fertility reduction, water and soil pollution, and increased greenhouse gas emissions, stemming from alterations in LULC (Hashimoto et al., 2004; Mostafazadeh & Talebi Khiavi, 2024). The upward trend in urban population and migration to urban life predominantly drives alterations in LULC within urban areas. Additionally, the adverse outcomes of unplanned urban development include the scarcity of suitable land for population settlement and increased pressure on limited environmental resources (Sarif & Gupta, 2022). It should be noted that influential factors affecting LULC changes in different temporal and spatial conditions have varying impacts on ecosystem performance and processes (Irwin & Geoghegan, 2001). LULC changes significantly affect various ecosystem functions, gaining substantial environmental importance, drawing attention from researchers and scientists worldwide (Mas et al., 2014; Schneider et al., 2020; Gul et al., 2021). Recent unplanned urban development has led to extensive alterations in urban LULC patterns, resulting in substantial environmental and socio-economic effects (Devi et al., 2022; Talebi Khiavi et al., 2022). Therefore, the primary challenge for urban planners lies in equitably distributing urban resources and services across various urban areas according to the societal needs of each urban community. Unsustainable LULC and alterations without considering environmental capacities disrupt environmental balance and challenge sustainable urban development (Ahmed et al., 2022). Effective land management, realistic modeling of urban development needs for land, evaluating influential variables for future land development, particularly in predicting residential land development and its effects, are essential endeavors (Zhan & Xie, 2022).

LULC is a consequence of human activities in ecosystem management. Predicting future LULC patterns can assist managers and policymakers in making informed decisions. Inappropriate land use practices, such as deforestation, extensive livestock farming, agricultural expansion, urban development, and city planning, threaten watershed conditions in different times and locations (Lambin et al., 2003). Simulating urban development using various models serves as a potent tool for predicting changes in urban areas (Al-sharif & Pradhan, 2015). Urban growth models, employing geographic information systems and remote sensing dynamically, help identify spatial trends and the intensity of changes in city development, allowing urban planners to manage urban growth considering natural environmental capabilities (Ullah & Wadood, 2020; Yang et al., 2020). Assessing temporal changes and spatial patterns in land use is crucial to establish a comprehensive environmental management pattern. Spatial models provide decision-making tools for planners and policymakers, aiding their understanding of urban development processes. Several studies have simulated specific urban physical growth and LULC changes. For instance, Aghaei et al. (2020) utilized three Landsat TM and ETM+ satellite images from 2000, 2010, and 2018 in the Kouzetopraghi watershed in Ardabil province to simulate and evaluate LULC changes. Zabihi et al. (2020) concluded continuous increases in agricultural land and residential areas led to deforestation and rangeland destruction in the Talar watershed in Mazandaran province. Khoshnood Motlagh et al. (2021) employed LCM and Markov methods to predict LULC changes in the Hableroud watershed in Iran's semi-arid region, achieving Kappa accuracy percentages of 75%, 78%, and 81% for the years 1986, 2000, and 2017, respectively.

Talebi Khiavi and Mostafazadeh (2021) aimed to evaluate the dynamic changes in LULC in the Khiavchi region using a supervised maximum likelihood classification method for the years 1984, 1992, 2000, 2008, and 2016. They found that residential areas exhibited the highest degree of change and a dynamic magnitude of 97.7%. Moreover, forest and rangeland usage experienced decreasing trends with dynamic indices of -1.85 and -2.37, respectively, over the 32-year period. Ozturk (2015) simulated urban development in Atakum, Turkey, using the MLP model and Markov chain, achieving a 35.2% urban growth during the years 2013 to 2025. Losiri and colleagues (2016), aiming to model urban development in the Bangkok metropolitan area, utilized the LCM module and MLP method to model the transfer potential and attained an overall model accuracy exceeding 90%. Their examination of land use maps for the years 1988, 1993, 1998, 2003, 2008, and 2011 emphasized the striking development of the Bangkok metropolitan area for future conditions. Wang and colleagues (2023) aimed to forecast land use changes in the Manasi region of China, utilizing land dynamic indices and land surface parameters. Their findings between 1990 and 2020 revealed an increase in agricultural lands, tree cover, water bodies, and urban areas, while rangelands and barren lands decreased. The MLP-LSTM model exhibited the highest accuracy, with a Kappa coefficient of 58.95%, in predicting land use changes. Lukas et al. (2023) assessed land use/land cover changes from 1991 to 2022 and projected future changes in the Omo-Gibe watershed in Ethiopia. They employed Landsat satellite imagery and a random forest machine learning algorithm for classification, achieving an overall accuracy of 86.53%. Their results indicated a significant increase in agricultural lands and shrublands alongside a reduction in forests and grasslands between 2022 and 2037. Nyatuame and colleagues (2023) aimed to analyze land use/land cover changes in the Tordzie watershed in Ghana using Landsat satellite images from 1987, 2003, and 2017, employing a supervised classification method. Their results showed a considerable increase in residential areas and agricultural lands, while vegetation cover had decreased. The expansion of agricultural lands by 2030 and 2050, forming 56% of the entire watershed, underscored the importance of proper resource management, land use policies, and sustainable practices.

Various models and methods exist for simulating and predicting LULC changes, among which include the DIANAMIC, CLUE, GEOMOD, and LCM modules. Among these, the LCM module has gained more popularity in modeling LULC changes due to its user-friendliness and diverse capabilities (Balha et al., 2020; Thiha et al., 2021). Different decisions, such as strategic choices, policies, implementation plans, design, and land potential assessments, require relevant models at various decision-making levels using Geographic Information Systems (GIS). In essence, models form the basis for spatial decision-making in GIS systems (Verburg et al., 2006). Environmental conditions, especially in specific locations, significantly influence urban development and its progression. In the northern regions of the country, particularly in Golestan province, the presence of Hyrcanian forests, fertile lands, and moderate climates make environmental conditions highly important. The city of Gorgan has faced rapid population growth and excessive physical development in recent years. Conducting a study and modeling the expansion trend of this city using the LCM method can aid in identifying the developmental trend. It can also compare it with existing comprehensive urban plans, facilitating the formulation of urban development plans and service provisions for citizens, which serves as a guide for urban planners (Saravanan et al., 2019). The selection of Gorgan as our case study stems from its unique geographical and socio-economic characteristics. Situated at the region of the Hyrcanian forests (a UNESCO World Heritage site) Gorgan encompasses diverse ecological zones, including plains, foothills, and mountainous areas. This diversity makes it an ideal location to study land use dynamics. In recent decades, Gorgan has experienced rapid urbanization, driven by migration from various regions, owing to its favorable climate and economic opportunities. This urban expansion has led to significant transformations in land use, notably the conversion of agricultural and forested lands into residential and commercial areas. Such changes pose challenges to sustainable development and environmental conservation. Gorgan, the capital of Golestan Province, has experienced rapid population growth and physical expansion in recent decades, driven by internal migration, strategic location, and favorable climate. While its proximity to forests, fertile lands, and water resources has supported agriculture and tourism, unregulated urban growth has caused extensive land-use changes, forest loss, and pressure on natural resources. Few studies have assessed land-use changes or future projections in this region, and most rely on single models, whereas combining LCM and Markov Chain can improve prediction accuracy.

This study addresses critical gaps in land-use change modeling and urban growth prediction in rapidly developing areas like Gorgan, where

environmental and socio-economic factors drive complex land dynamics. By integrating the Land Change Modeler (LCM), Markov Chain analysis, and machine learning algorithms (SVM and MLP), the research analyzes land-use trends from 1991 to 2021 and projects future changes up to 2051. The combined use of multi-temporal satellite imagery and diverse features, spectral, textural, and phenological, enhances classification accuracy in heterogeneous landscapes. Special attention is given to key transitions, particularly the conversion of irrigated farmland to residential and orchard land, which carries important implications for ecological security, food systems, and water resources. This integrated framework significantly improves spatial prediction accuracy and offers valuable insights into the pace and intensity of urban expansion. The aim of this research is to model land-use changes and predict the future spatial development of Gorgan, a city in north-eastern Iran, with conditions of rapid population growth and physical expansion. This study utilizes the simultaneous combination of Land Change Modeler (LCM) and Markov Chain models with remote sensing data and advanced machine learning algorithms (SVM and MLP) to enhance the accuracy of land-use change and urban development predictions. In addition to analyzing past trends (1991-2021), this research also predicts land-use changes until 2051. The results provide indications for urban planning and policy-making, ensuring Gorgan's growth aligns with environmental sustainability and preserves its natural forests.

2 MATERIAL AND METHODS

Study Area

The county of Gorgan covers approximately 8% of Golestan Province's surface area, spanning about 1615 square kilometers. This county is divided, according to national divisions, into two regions: Central and Baharan, encompassing four cities: Gorgan, Jelin, Sorkhankolateh, and Garg. Gorgan region borders Aghghala and Bandar Torkaman counties to the north, Semnan Province to the south, Aliabad-katool County to the east, and Kordkoi County to the west. According to the 2016 population and housing census, the population of Gorgan region is estimated at 480,541 individuals, constituting approximately 35% of the province's total population. The relative population density in Gorgan region (259 individuals per square kilometer) is three times higher than that of Golestan Province (83 individuals per square kilometer). The average annual precipitation in the researched area is around 577 millimeters, and the annual average temperature, based on meteorological station statistics in Gorgan, is recorded at 17.8 degrees Celsius.

Methodology

In order to conduct the present research, satellite images from ETM+ and OLI sensors were acquired from the United States Geological Survey website to prepare land-use maps for the years 1991, 2006, and 2021. Details of the satellite images used in this study are presented in Table 1. The selection of these satellite images was based on the maximum vegetation coverage on the Earth's surface and the least cloud cover. Additionally, for the years under study, Google Earth imagery (© Google Earth, Image © 1991 Landsat, 2006 Landsat, 2021Landsat/Copernicus) was used to understand the regional conditions and to validate some of the land use classifications in the study area. The Digital Elevation Model (DEM) was one of the fundamental bases for generating base maps, including slope, which was created using ArcGIS 10.8.2 software. Additionally, the canal and road network map was extracted from the topographic map with a scale of 1:25,000 within the study area.

Tab. 1. Specifications of satellite images used in predicting LULC changes in Gorgan region

Period	Date	Satellite/ Sensor	Row-path
1991	June 04 1991	Landsat 5/TM	162-035
2006	Aug 22 2006	Landsat 5/TM	162-035
2021	June 20 2021	Landsat 7/ETM+	162-035

Pre-processing of Satellite Images

To enhance the accuracy of satellite image processing and ensure the quality of input data, pre-processing methods were employed in this study. The FLAASH method, recognized as one of the most accurate algorithms for atmospheric correction of satellite images, significantly reduced atmospheric errors by considering various atmospheric parameters such as water vapor and aerosols (Adler-Golden et al., 1998). For the current study, atmospheric correction of the research satellite images was performed using the Fast Line of Sight Atmospheric Analysis of Spectral Hypercubes (FLAASH) method within the ENVI 5.3 software environment (Feizizadeh, 2017; Rozenstein & Karnieli, 2011). Radiometric correction of the images utilized in the study was executed through the Radiometric Calibration command (Zabihi et al., 2020). Moreover, the application of the radiometric calibration method eliminated disturbances arising from sensor variances and imaging conditions.

Training Sample Collection and LULC Classification

LULC identification based on color differences involved employing False Color Composite (FCC) images, combining spectral values of green, red, and near-infrared bands (Khoi & Murayama, 2010). Initially, supervised classification necessitates defining regions used as training samples for each land-use category (Eastman, 2015). Training samples representing different land-use categories were gathered through field surveys, utilization of Google Earth imagery, and visual interpretation of false-color composite images (Rafiee et al., 2009; Chen et al., 2011). Eight LULC categories were identified in the study area, encompassing forest, rangeland, irrigated farming, dry farming, residential areas, water bodies, orchards, and rocky terrains. Eight LULC categories were selected to represent the dominant land uses and environmental diversity of the study area. They capture key ecological, agricultural, and human systems essential for land change analysis. Grouping into major types improved classification accuracy and interpretability, and aligns with previous studies and research objectives.

Table 2 presents the major land use/land cover (LULC) classes identified in the study area, including detailed descriptions and representative examples for each category.

The classification of Landsat satellite images in the research years was conducted using the supervised Support Vector Machine (SVM) method. The selection of the SVM classification method, due to its strong capability in separating data with complex boundaries and its ability to handle nonlinear data, significantly improved the classification accuracy (Thanh Noi & Kappas, 2018).

Compared to other conventional methods such as Maximum Likelihood, SVM is less sensitive to

Tab. 2. Explanation of the different LULC classes identified in the study area along with descriptions

LULC Class	Explanation	Example
Dry Farming	Areas used for agriculture where crops are grown without irrigation, relying on natural rainfall.	Wheat and Barley, Dry Wheat and Soybean
Forest	Areas covered with trees, including natural forests and plantations.	Beech, Ash, Oak, Hornbeam, Zurbine, Yew, Maple, Sycamore
Irrigated Farming	Agricultural land that is irrigated to support crops, often in regions with water availability.	Irrigated Wheat, Irrigated Barley, Cotton, Rice, Canola, Sunflower, Sugar Beet
Orchards	Areas dedicated to the cultivation of fruit trees or nut trees.	Citrus, Peach, Apple, Plum, Pear, Cherry
Rangeland	Land used for grazing livestock, often characterized by natural vegetation or grasslands.	Steppe and Semi-steppe Rangelands
Residential Area	Urban or suburban areas where people live, consisting of homes, apartments, and related infrastructure.	Residential and Urban Areas
Rock	Land areas covered by rocks, often with minimal soil or vegetation.	Mountainous Areas, Rocky Outcrops, Mountain Ridges
Water Body	Areas covered by water, such as rivers, lakes, reservoirs, or wetlands.	Natural or man-made water bodies

the number of training samples and performs better with data exhibiting high spectral overlap (Shao & Lunetta, 2012). SVM was chosen for its high accuracy in classifying diverse land cover types, particularly effective in complex landscapes like the study area (Saadat et al., 2011; Alizadeh et al., 2018). Its ability to process large, high-dimensional datasets ensures precise LULC mapping, making it ideal for change analysis (Kavzoglu & Colkesen, 2009). In the process of distinguishing between LULC classes, in addition to the spectral characteristics of the images (reflectance values of different bands), spectral indices such as NDVI, and textural features were utilized to enhance class separability (Naboureh et al., 2020). Furthermore, the seasonal behavior (phenology) of the covers was considered to better differentiate classes such as irrigated and rainfed agriculture or orchards and natural forests. A total of 655 samples were collected across the Gorgan region for all land-use categories. Of these, 458 were used for training the classification algorithm, and 197 were allocated for accuracy assessment. The samples were selected to ensure an appropriate spatial distribution throughout the region and to cover environmental diversity, including intra-class variations such as differences in vegetation density between dense and sparse forests, variations in the size and pattern of irrigated and rainfed farms, and other visual characteristics (Li et al., 2021). This approach ensured that the collected samples not only served as suitable representatives for each land use/land cover class but also effectively reflected the natural heterogeneity of the area. The number of samples assigned to each class was determined based on the class area and its internal heterogeneity, ensuring a balanced distribution of training and validation data.

Accuracy Assessment of the Classified Maps

For the accuracy assessment of the classified maps, the error matrix was extracted (Fang et al., 2006). The Overall Accuracy and Kappa Coefficient indices were calculated based on Equations (1) to (3) (Nehzak et al., 2022; Dehghani et al., 2023).

$$\text{Overall Accuracy} = \frac{\sum_{i=1}^{k} X_{ii}}{N} \times 100\% \quad (1)$$

where X_{ii} is the number of samples correctly classified in class i, k is the total number of LULC classes, and N is the total number of evaluated samples (the sum of all elements in the error matrix).

$$\text{Kappa} = \frac{P_0 - P_e}{1 - P_e} \quad (2)$$

where Po represents the overall accuracy or the proportion of trials in which judges agree, and Pe is the expected random accuracy or the proportion of trials in which agreement would be expected due to chance. Meanwhile, Pe is calculated using Equation 3.

$$P_0 = \sum_{i=1}^{k} \left(\frac{X_{i+} \times X_{+i}}{N^2} \right) \quad (3)$$

where $Xi+$ is the sum of row i (total actual samples in class i), and $X+i$ is the sum of column i (total predicted samples in class i). The analysis of the accuracy assessment results indicated that the methods employed in this study, due to the use of advanced preprocessing and classification techniques, successfully produced land use/land cover maps with acceptable accuracy and minimal classification error.

Modeling transfer potential and predicting LULC changes

For modeling LULC changes and predicting future conditions, a land change model was employed. The modeling was executed using the Land Change Modeler (LCM) in three stages, comprising change analysis, potential transition modeling, and LULC change prediction, employing MLP and Markov Chain methods. The models incorporated key variables including proximity to forests, residential areas, and roads, with their accuracy verified through training and test error coefficients, yielding reliable results consistent with the region's actual conditions.

LCM was selected for modeling spatial transitions between land-use classes over time, enabling both historical analysis and future projections (Zabihi et al., 2020; Singh et al., 2022). In the current study, two periods, namely 1991 to 2006 and 2006 to 2021, were respectively considered as calibration and validation periods. The periods 1991–2006 and 2006–2021 were chosen for their high-quality satellite data, alignment with prior studies, and expert knowledge of land-use dynamics. Despite slight differences from future intervals, the 15-year spans support robust Markov-based modeling. Rigorous calibration and accuracy assessments, including Cramer's V and the Kappa index, minimized any potential effects. Reductions and increments in each LULC category, net changes in LULCs, the contribution of different LULC categories in the increase or decrease of a specific LULC category, LULC change maps during the study periods, unchanged areas map, and spatial trend map of LULC changes were developed during the LULC change analysis phase (Nagabhatla et al., 2008; Václavík & Rogan, 2009; Mas et al., 2014). During the

potential transition modeling phase, the transition potential from one LULC type (such as forest) to another (such as agriculture) is modeled based on descriptive and influential variables (e.g., distance from agricultural lands, proximity to residential areas, etc.). It is essential to note that for selecting sub-models with the highest accuracy, it's necessary to run the transition potential model multiple times with different scenarios (Lin et al., 2014). In the current research, seven sub-models were developed for potential transition modeling using the Multilayer Perceptron (MLP) method. These sub-models were constructed considering variables like digital elevation model, distance from forest lands, distance from residential areas, distance from rangelands, distance from dry farming lands, distance from rivers, and distance from roads between the years 1991 to 2006 (the calibration period) (Yeh & Li, 2002; Monteiro et al., 2011; Sangermano et al., 2012). The LULC transition sub-models involved transitions from forest lands to rangelands, forest lands to irrigated farming lands, forest lands to dry farming lands, forest lands to residential areas, rangelands to irrigated farming lands, rangelands to dry farming lands, rangelands to residential areas, irrigated farming lands to orchards, and irrigated farming lands to orchards.

The Multilayer Perceptron is a non-parametric algorithm capable of explaining complex relationships between a set of variables and a set of outputs, even in cases where there is collinearity among the variables (Lin et al., 2014). To select influential variables, Cramer's V coefficient was utilized, demonstrating the degree of association between the variables and land use changes (Munsi et al., 2012). Variables with Cramer's coefficient around or exceeding 0.15 and 0.4 are respectively considered useful and robust (Eastman, 2015). The Markov Chain method complements this by providing probabilistic transition modeling, reliable for gradual changes and long-term predictions. Together, they offer robust tools for multi-scale land-use change studies (Singh et al., 2018). The evaluation of the potential transition modeling method was conducted using the accuracy criterion. LULC change predictions were made using the Markov Chain method (Hussain et al., 2024). It's noteworthy that based on maps from 1991 and 2006, a map for 2021 was forecasted. Subsequently, maps for 2036 and 2051 were predicted based on LULC maps from 2006 and 2021 using the LCM environment.

The models predict future changes using historical land-use data, validated through a two-step process: calibration (1991–2006) and validation (2006–2021). Transition potential was tested under multiple scenarios, while map accuracy (2021–2051) was verified using the Kappa index. Furthermore, the use of influential variables, selected through statistical methods such as Cramer's V coefficient, strengthens the credibility of the predictions (Dzieszko, 2014; Alqadhi et al., 2021). While uncertainties in land-use projections exist, the methodology employed has been rigorously tested and proven effective in similar studies.

The evaluation of the predicted LULC map was carried out using the Kappa index, employing the Validate command in the TerrSet software for this purpose.

3 RESULTS

The results depicting LULC maps for the years 1991, 2006, and 2021 are presented in Figure 1, while the respective areas and percentages pertaining to each LULC category for the studied years are shown in Table 3.

Based on the results presented in Figure 1 and Table 3, forest LULC is identified as the predominant LULC category in Gorgan region, which has experienced an annual decrease of 0.09% from 1991 to 2021. Furthermore, the research findings indicate a reduction of 5.31% and 2.53% in Irrigated farming lands during the study period (Table 3).

After determing the LULC categories for the study years in the study area, the the accuracy assessment results of satellite image classification and the prepared LULC maps, utilizing Kappa coefficient and overall accuracy, are presented in Table 4

Tab. 4. The results of evaluating the accuracy of LULC maps in the years of research in Gorgan region

Year	Kappa index	Overall accuracy (%)
1991	0.67	72.6
2006	0.7	75.1
2021	74.5	78.2

The net changes, reductions, and increments in each LULC category within the study area of Gorgan region during the research period (1991 to 2021) are illustrated in Figure 2.

Figure 3 displays the map of unchanged LULC areas between 1991 and 2021, and the spatial pattern of changes from other LULC categories to the residential area within the study boundary of Gorgan region.

According to Figure 3, between 1991 and 2021, much of the study area maintained its primary land cover, with forests in the north and rangelands in the south remaining largely stable.

The results obtained from examining the relationship between influential factors affecting LULC changes and continuous occurrences in the study region, using Cramer's V coefficient, are displayed in Table 5.

Tab. 3. Area (square kilometers) and percentage of each LULC class in the study years in Gorgan region

LULC Class	1991		2006		2021	
	area	%	area	%	area	%
Dry Farming	46.2	2.95	63.44	4.05	88.33	5.64
Forest	586.34	37.44	584.07	37.29	583.47	37.26
Irrigated Farming	513.44	32.78	430.31	27.48	390.68	24.95
Orchards	22.06	1.41	29.72	1.9	65.72	4.2
Rangeland	346.85	22.15	366.08	23.37	339.49	21.68
Residential Area	29.37	1.88	73.85	4.72	77.64	4.96
Rock	21.49	1.37	18.37	1.17	18.98	1.21
Water Body	0.34	0.02	0.25	0.02	1.79	0.11
Sum	1566.099	100	1566.099	100	1566.099	100

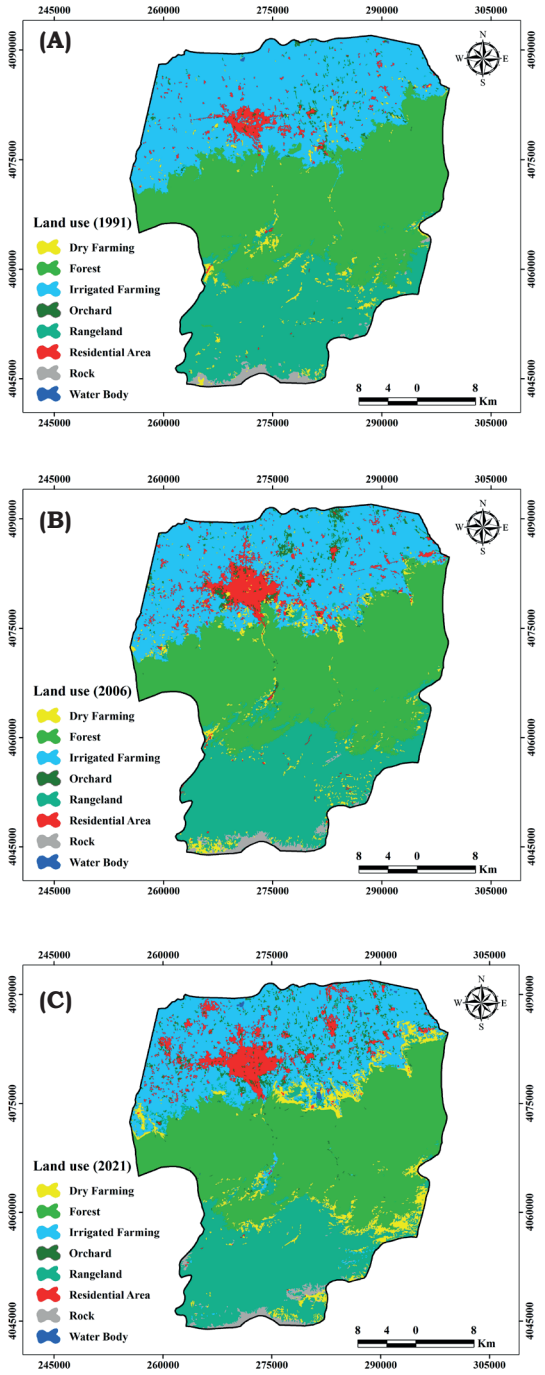

Fig. 1. LULC maps for the years a) 1991, b) 2006 and c) 2021

Tab. 5. The degree of correlation between the factors affecting LULC change and the changes taking place using Kramer's coefficient

Factor	Training	Validation
Elevation	0.47	0.45
Distance to road	0.29	0.24
Distance to river	0.39	0.29
Distance to forest	0.41	0.37
Distance to rangeland	0.36	0.32
Distance to residential area	0.28	0.25
Distance to dry farming	0.37	0.33

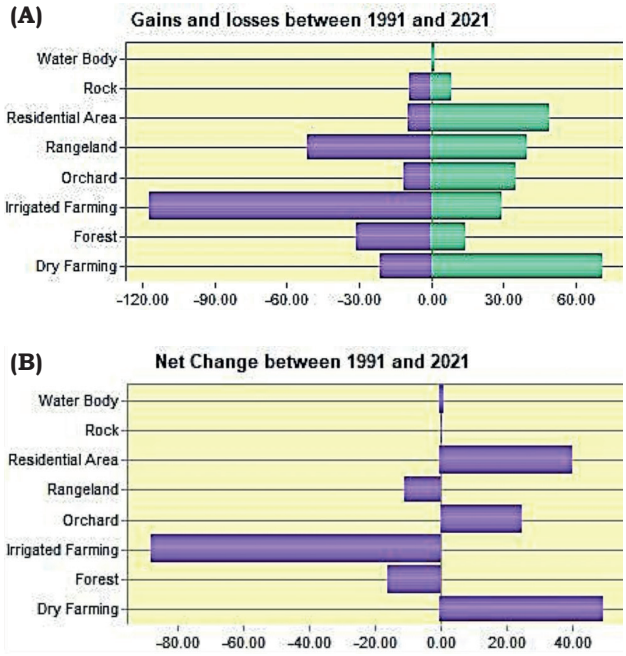

Fig. 2. Gains and losses (a), and net changes (b), of different LULC classes (square kilometers) during the study period in Gorgan region

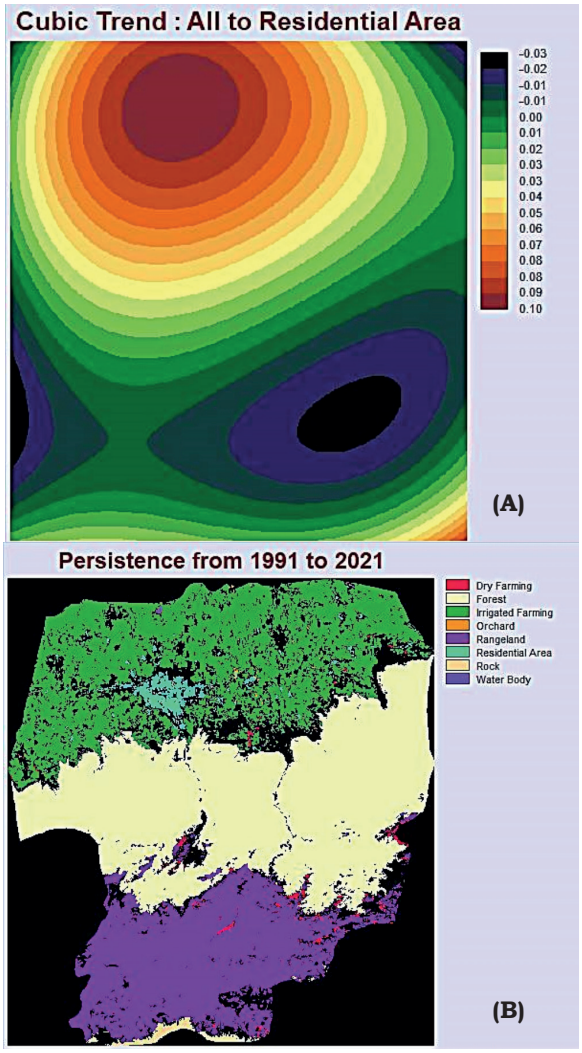

Fig. 3. The spatial trend of change from other LULCs to residential area use (a), and areas without LULC change (b), during the study period in Gorgan region

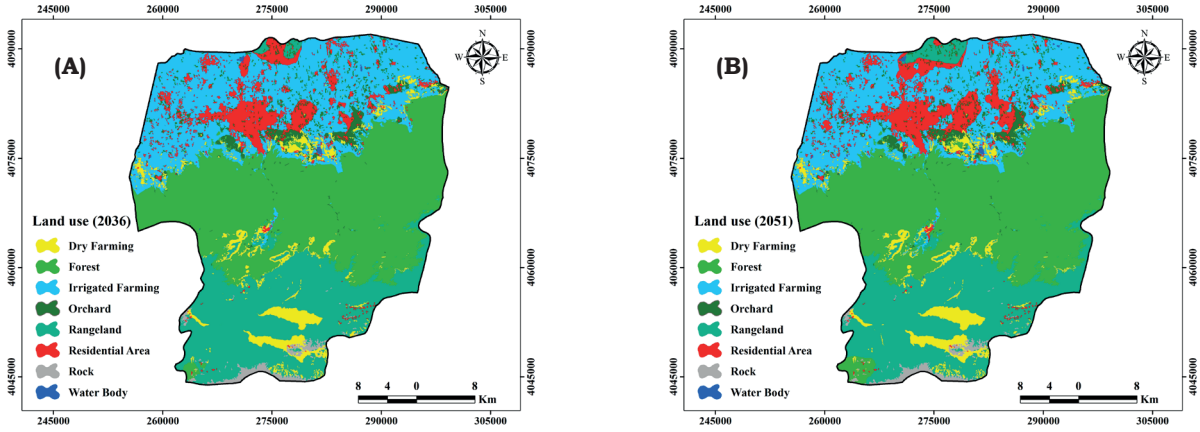

Fig. 4. Predicted LULC map in 2036 (a), and 2051 (b) of Gorgan region using LCM

Projected LULC maps for 2036 and 2051 using the Multilayer Perceptron and Markov Chain in the Land Change Modeler (LCM) framework are depicted in Figure 4. Findings related to the area and percentage of various predicted LULC categories within the study boundaries of Gorgan region for the years 2036 and 2051 are outlined in Table 6.

According to Table 6, between 2036 and 2051 in the Gorgan region, dry farming, forest, and irrigated farming areas are predicted to slightly decline. Residential areas show a notable increase from 6.57% to 7.48%. Orchard areas are expected to grow, while rangeland remains relatively stable. The total land area remains unchanged at 1566.09 km².

4 DISCUSSION

According to Figure 1 and Table 3, notably, residential areas have shown an annual increase rate of 1.3% from 1991 to 2021. Moreover, the expansion of residential areas reached 44.48 and 3.78 square kilometers from 1991 to 2006 and 2006 to 2021, respectively, in Gorgan region. Additionally, orchards exhibited an annual increase of 1.39%, and dry farming showed an annual rise of 1.34% during the study years.

According to the findings presented in Figure 2, Irrigated farming and rangeland LULCs have decreased by 115 and 45 square kilometers, respectively, throughout the study period. Furthermore, dry farming and residential areas have increased by 75 and 40 square kilometers, respectively, during the research duration from 1991 to 2021. Regarding the net changes in various LULC categories in Gorgan region, it should be noted that between 1991 and 2021, the maximum decrease in net change corresponds to Irrigated farming by an equivalent of 90 square kilometers, while the maximum increase in net change is attributed to dry farming and residential areas, totaling 70 and 40 square kilometers, respectively. Our results demonstrate a persistent decline in forest cover (-0.09% annually) and irrigated farmland (-5.31% total) alongside rapid urban expansion (+1.3% annually) in Gorgan. The Hyrcanian forests' vulnerability mirrors findings in biodiversity hotspots like Sumatra (Linkie et al., 2008), though our MLP-Markov approach captured finer transition dynamics (e.g., irrigated to orchards) often overlooked in broad-scale studies.

As shown in Figure 3, however, scattered red areas, especially in dryland farming and rangelands, indicate localized changes. These align with high values on the "Cube Trend: Change to Residential" map, pointing to specific zones of land conversion. The trend map highlights residential expansion hotspots, marked by dark red and brown areas, indicating urban or semi-urban growth. Overall, the maps show general LULC stability with spatially uneven but notable residential development in certain areas.

According to the findings in Table 5, the elevation factor above sea level, with Cramer's V values of 0.47 and 0.45 respectively for the validation and verification periods, has exerted the greatest impact on LULC changes in Gorgan region. It's noteworthy that this factor has an effect on variables such as slope, natural LULCs like forests and rangelands, and accessibility to infrastructure, significantly influencing the trends and extent of LULC changes. The importance of these variables in modeling LULC changes has also been emphasized in other studies (Dendoncker et al., 2007; Li & Yeh, 2002; Monteiro et al., 2011; Verburg et al., 2002; Mas et al., 2004). For instance, proximity to roads, cities, and forest/non-forest margins in Southern Cameroon were reported

Tab. 6. Predicted values of area (square kilometers) and percentage of different LULC classes in 2036 and 2051 in Gorgan region

LULC Class	2036		2051	
	area	%	area	%
Dry Farming	74	4.73	73.41	4.69
Forest	580.3	37.05	576.84	36.83
Irrigated Farming	390.14	24.91	368.43	23.53
Orchards	66.63	4.25	76.52	4.89
Rangeland	331.18	21.15	332.81	21.25
Residential Area	102.9	6.57	117.14	7.48
Rock	19.33	1.23	19.32	1.23
Water Body	1.6	0.1	1.6	0.1
Sum	1566.09	100	1566.09	100

as essential variables in modeling forest changes (Lambin, 1997). Similarly, height and proximity to roads were significant factors in forest changes in lowland Sumatra (Linkie et al., 2008). Schulz et al.'s study in 2011 also demonstrated that slope and proximity to main roads significantly affect vegetation cover changes in Chile.

The outcomes of the current research regarding the evaluation of transfer potential modeling using the MLP method indicate training and test errors of 0.20 and 0.21, respectively, during the validation period. The accuracy level of the transfer potential modeling method in the LCM approach for Gorgan region's study area reached 78.70%.

Considering the forecasted results of LULC areas for Gorgan region using the LCM module as presented in Table 6, it can be inferred that in the year 2036, orchards and residential areas will experience an increase in their land areas compared to 2021. Conversely, forested areas, irrigated farming, and rangelands are expected to witness a decrease in their land areas. Similar trends in LULC changes for the year 2051 compared to 2036 are anticipated (Figure 4).

The utilization of the LCM module has been identified in various studies such as Gholamalifard et al. (2013), and Azizi Ghalati et al. (2013) due to its high precision, making it a suitable technique for monitoring and predicting urban development and LULC changes. The accuracy assessment of the Transfer Potential Modeling using the MLP model demonstrated high precision across most sub-models, aligning with the results of Gholamalifard et al. (2013), indicating high accuracy ranging from 52% to 93% in most sub-models. The findings of the current research affirm the high accuracy of the chosen model, with approximately 95% accuracy for each selected sub-model.

The employment of MLP through framework achieved higher accuracy (Kappa=0.85) than standalone Markov implementations (e.g., Khoshnood Motlagh et al., 2021: Kappa=0.81). Our elevation-driven transition model (Cramer's V=0.47) outperforms distance-based models in similar terrains (e.g., Monteiro et al., 2011), likely due to DEM-derived slope integration, a critical factor in mountainous watersheds (Schulz et al., 2011). However, the 21% test error highlights limitations in modeling abrupt anthropogenic changes (e.g., policy-driven land conversions).

The predicted 7.48% urban expansion by 2051 exceeds growth rates in comparable Iranian cities, reflecting Gorgan's role as a regional migration hub. The orchard expansion (+4.89% by 2051) contrasts with Mediterranean studies showing agricultural abandonment (Dendoncker et al., 2007), emphasizing regional economic dependencies on perennial crops. The evaluation of predicted LULC maps for the year 2021 against the actual ground-truth maps during the validation period showed overall Kappa, location agreement, and quantity agreement scores of 0.85, 0.88, and 0.83, respectively. These accuracy assessment results indicate a high precision of the model in predicting LULC maps for the years 2036 and 2051.

Contributions

The MLP-based transition modeling demonstrates superior handling of complex variable interactions, evidenced by low training (0.20) and test (0.21) errors - a technical improvement over conventional logistic regression methods. The incorporation of Cramer's V coefficient analysis quantitatively validates that elevation (V=0.47) and hydrological proximity (V=0.39) are dominant drivers of LULC changes in Hyrcanian ecosystems, addressing a knowledge gap in northern Iran's landscape dynamics. The identification of non-linear urbanization patterns shows acceleration in residential expansion (1.3% annual increase) post-2006. The results found that agricultural intensification follows a cascade pattern-irrigated farms (-7.83% decline) preferentially convert to orchards (+2.79% gain) rather than residential areas, revealing unique land-use succession pathways. Using 30 years of multi-temporal satellite data, the research provides a detailed view of spatial development trends. It assesses classification accuracy (Kappa, overall accuracy) and analyzes drivers of change using Cramér's V. The projected land use maps for 2036 and 2051 offer strategic insights for urban planning and natural resource management. Focusing on a sensitive area like the Hyrcanian forests adds ecological value, and the findings show accelerated urban growth from 2006 to 2021. The study presents a generalizable framework for modeling land use change in similar developing regions.

Limitations and implications

Cloud cover in Landsat imagery may underrepresent seasonal land uses. Future studies should integrate Sentinel-2 for higher temporal resolution. Incorporating socioeconomic drivers (e.g., migration rates) could improve transition rules beyond biophysical factors. Our 2036/2051 projections highlight urgent needs for Greenbelt policies to protect Hyrcanian forests, water-efficient agriculture incentives given irrigated land losses and Compact urban growth strategies to minimize rangeland fragmentation.

The study delivers three actionable indications for regional management: (1) The spatial change trend maps (Fig. 3) identify high-risk forest conversion zones, enabling targeted conservation in the southeastern study area. (2) Our documented 5.31% loss of irrigated farmland signals urgent need for agricultural land protection policies. (3) The 78.2% map accuracy achieved using freely available Landsat data provides a cost-effective framework for resource-limited municipalities.

Our peri-urban analysis reveals distinct dynamics: slower but steadier forest conversion (0.09% annual loss) and orchard-oriented agricultural transitions unseen in arid regions. The 30-year validation period (1991-2021) exceeds typical short-term spans in comparable studies, enhancing model reliability for long-term planning.

5 CONCLUSIONS

The monitoring and forecasting of temporal and spatial changes in urban areas due to population growth and the preservation of ecosystem services, while minimizing their adverse effects on the environment, have become a focal point of scientific research and managerial efforts. The utilization of multi-temporal satellite images can serve as foundational data for analyzing spatial information related to LULC changes. The objective of this study is to model LULC changes, emphasizing human-made LULCs, particularly residential areas in Gorgan region, and forecast them for future conditions using the Land Change Modeler (LCM). The results of LULC changes in the study area revealed that LULC categories such as residential areas, orchards,

and dry farming exhibited an increasing trend from 1991 to 2021, while forested areas, irrigated farming, and rangelands depicted a decreasing trend during the same period. Moreover, these changes in the forecasting period (2021 to 2036 and 2036 to 2051) followed a similar pattern. The residential land-use category showed continuous growth over the 30-year period (1991 to 2021), indicating the developmental trend of Gorgan region, notably more significant between 2006 and 2021 compared to 1991 to 2006. Based on LULC change predictions in Gorgan region using the LCM module, it is projected that forested lands and rangelands will continue to decrease compared to 2021, while orchards and residential areas will experience an upward trend. In essence, LULC changes in the forecasting period were in line with the modeling period for dry farming, orchards, and residential areas. Factors influencing LULC changes, as considered in this study (elevation, distance from rangelands, distance from residential areas, distance from dry farming areas, distance from rivers, and distance from forests), are commonly utilized in predicting LULC changes in various studies. Among these variables, the distance from rangelands had the most significant effect, while the distance from roads had the least impact on the LULC change pattern in the study area. Azizi Ghalati et al. (2014), have also highlighted the importance of such factors in predicting LULC changes. Predicting LULC considering influential factors can assist various executive sectors in water and soil resource management, facilitating informed decision-making in formulating management policies. Knowledge about the trends, intensity, and potential spatial maps for different LULC types can aid in future land management planning. The predicted future LULC maps can serve as a basis for forecasting the desirable and undesirable consequences and impacts of land cover/use changes in the future.

REFERENCES

Adler-Golden, S., Berk, A., Bernstein, L. S., Richtsmeier, S., Acharya, P. K., Matthew, M. W., Anderson, G. P., Allred, C. L., Jeong, L. S., & Chetwynd, J. H. (1998). FLAASH, a MODTRAN4 atmospheric correction package for hyperspectral data retrievals and simulations. In Proc. 7th Ann. JPL Airborne Earth Science Workshop (Vol. 97, pp. 9–14). Pasadena, CA: JPL Publication. https://aviris.jpl.nasa.gov/proceedings/workshops/98_docs/2.pdf

Aghaei, M., Khavarian, H., & Mostafazadeh, R. (2020). Prediction of Land Use Changes Using the CA-Markov and LCM Models in the Kozehtopraghi Watershed in the Province of Ardabil. Watershed Management Research Journal, 33(3), 91–107. https://doi.org/10.22092/wmej.2019.128009.1267

Ahmed, N., Wang, G., Booij, M. J., Xiangyang, S., Hussain, F., & Nabi, G. (2022). Separation of the impact of landuse/landcover change and climate change on runoff in the upstream area of the Yangtze River, China. Water Resources Management, 36(1), 181–201. https://doi.org/10.1007/s11269-021-03021-z

Alizadeh, P., Kamkar, B., Shataee, S., & Kazemi Posht Masari, H. (2018). Estimation of changes in land area under wheat and soybean cultivation using satellite images classification techniques in west of Golestan province. Applied Field Crops Research, 31(3), 41–61. https://doi.org/10.22092/aj.2018.121231.1268

Alqadhi, S., Mallick, J., Balha, A., Bindajam, A., Singh, C. K., & Hoa, P. V. (2021). Spatial and decadal prediction of land use/land cover using multi-layer perceptron-neural network (MLP-NN) algorithm for a semi-arid region of Asir, Saudi Arabia. Earth Science Informatics, 14(3), 1547–1562. https://doi.org/10.1007/s12145-021-00633-2

Al-sharif, A. A., & Pradhan, B. (2015). A novel approach for predicting the spatial patterns of urban expansion by combining the chi-squared automatic integration detection decision tree, Markov chain and cellular automata models in GIS. Geocarto International, 30(8), 858–881. https://doi.org/10.1080/10106049.2014.997308

Azizi Ghalati, S., Rangzan, K., Taghizadeh, A., & Ahmadi, S. (2014). LCM Logistic regression modelling of land-use changes in Kouhmare Sorkhi, Fars province. Iranian Journal of Forest and Poplar Research, 22(4), 585–596. https://doi.org/10.22092/ijfpr.2015.13174

Balha, A., Vishwakarma, B. D., Pandey, S., & Singh, C. K. (2020). Predicting impact of urbanization on water resources in megacity Delhi. Remote Sensing Applications: Society and Environment, 20, 100361. https://doi.org/10.1016/j.rsase.2020.100361

Chen, Y., Li, X., Zheng, Y., Guan, Y., & Liu, X. (2011). Estimating the relationship between urban forms and energy consumption: A case study in the Pearl River Delta, 2005–2008. Landscape and Urban Planning, 102(1), 33–42. https://doi.org/10.1016/j.landurbplan.2011.03.007

Dehghani, T., Ahmadpari, H., & Amini, A. (2023). Assessment of land use changes using multispectral satellite images and artificial neural network. Water and Soil Management and Modelling, 3(2), 18–35. https://doi.org/10.22098/mmws.2022.11279.1114

Dendoncker, N., Rounsevell, M., & Bogaert, P. (2007). Spatial analysis and modelling of land use distributions in Belgium. Computers, Environment and Urban Systems, 31(2), 188–205. https://doi.org/10.1016/j.compenvurbsys.2006.06.004

Devi, A. B., Deka, D., Aneesh, T. D., Srinivas, R., & Nair, A. M. (2022). Predictive modelling of land use land cover dynamics for a tropical coastal urban city in Kerala, India. Arabian Journal of Geosciences, 15(5), 399. https://doi.org/10.1007/s12517-022-09735-7

Dzieszko, P. (2014). Land-cover modelling using Corine Land Cover data and multi-layer perceptron. Quaestiones Geographicae, 33(1), 5–22. https://doi.org/10.2478/quageo-2014-0004

Eastman, J. R. (2015). TerrSet liberaGIS. Geospatial Monitoring and Modeling System. Manual. (pp. 340). https://s45055.pcdn.co/centers/geospatial-analytics/www-content/blogs.dir/7/files/sites/354/2024/11/Terrset-liberaGIS-Manual.pdf

Fang, S., Gertner, G., Wang, G., & Anderson, A. (2006). The impact of misclassification in land use maps in the prediction of landscape dynamics. Landscape Ecology, 21(2), 233–242. https://doi.org/10.1007/s10980-005-1051-7

Feizizadeh, B. (2017). Modeling the Trends of the Land Use/Cover Change and Its Impacts on the Erosion System of the Allavian Dam Based on the Remote Sensing and GIS Techniques. Hydrogeomorphology, 4(11), 21–38. https://dor.isc.ac/dor/20.1001.1.23833254.1396.4.11.2.3

Gholamalifard, M., Joorabian Shooshtari, S., Hosseini Kahnuj, S. H., & Mirzaei, M. (2013). Land cover change modeling of coastal areas of Mazandaran Province using LCM in a GIS environment. Journal

of Environmental Studies, 38(4), 109–124. https://doi.org/10.22059/jes.2013.29867

Gul, E., Riva, L., Nielsen, H. K., Yang, H., Zhou, H., Yang, Q., ... & Fantozzi, F. (2021). Substitution of coke with pelletized biocarbon in the European and Chinese steel industries: An LCA analysis. Applied Energy, 304, 117644. https://doi.org/10.1016/j.apenergy.2021.117644

Hashimoto, H., Nemani, R. R., White, M. A., Jolly, W. M., Piper, S. C., Keeling, C. D., Myneni, R. B., & Running, S. W. (2004). El Niño–Southern Oscillation–induced variability in terrestrial carbon cycling. Journal of Geophysical Research: Atmospheres, 109(D23). https://doi.org/10.1029/2004JD004959

Hussain, S., Mubeen, M., Nasim, W., Mumtaz, F., Abdo, H. G., Mostafazadeh, R., & Fahad, S. (2024). Assessment of future prediction of urban growth and climate change in district Multan, Pakistan using CA-Markov method. Urban Climate, 53, 101766. https://doi.org/10.1016/j.uclim.2023.101766

Irwin, E. G., & Geoghegan, J. (2001). Theory, data, methods: developing spatially explicit economic models of land use change. Agriculture, Ecosystems & Environment, 85(1–3), 7–24. https://doi.org/10.1016/S0167-8809(01)00200-6

Kavzoglu, T., & Colkesen, I. (2009). A kernel functions analysis for support vector machines for land cover classification. International Journal of Applied Earth Observation and Geoinformation, 11(5), 352–359. https://doi.org/10.1016/j.jag.2009.06.002

Khoi, D. D., & Murayama, Y. (2010). Forecasting Areas Vulnerable to Forest Conversion in the Tam Dao National Park Region, Vietnam. Remote Sensing, 2(5), 1249–1272. https://doi.org/10.3390/rs2051249

Khoshnood Motlagh, S., Sadoddin, A., Haghnegahdar, A., Razavi, S., Salmanmahiny, A., & Ghorbani, K. (2021). Analysis and prediction of land cover changes using the land change modeler (LCM) in a semiarid river basin, Iran. Land Degradation & Development, 32(10), 3092–3105. https://doi.org/10.1002/ldr.3969

Lambin, E. F. (1997). Modelling and monitoring land-cover change processes in tropical regions. Progress in Physical Geography: Earth and Environment, 21(3), 375–393. https://doi.org/10.1177/030913339702100303

Lambin, E. F., Geist, H. J., & Lepers, E. (2003). Dynamics of land-use and land-cover change in tropical regions. Annual Review of Environment and Resources, 28, 205–241. https://doi.org/10.1146/annurev.energy.28.050302.105459

Li, C., Ma, Z., Wang, L., Yu, W., Tan, D., Gao, B., Feng, Q., Guo, H., & Zhao, Y. (2021). Improving the accuracy of land cover mapping by distributing training samples. Remote Sensing, 13(22), 4594. https://doi.org/10.3390/rs13224594

Li, X., & Yeh, A. G. (2002). Neural-network-based cellular automata for simulating multiple land use changes using GIS. International Journal of Geographical Information Science, 16(4), 323–343. https://doi.org/10.1080/13658810210137004

Lin, L., Sills, E., & Cheshire, H. (2014). Targeting areas for Reducing Emissions from Deforestation and forest Degradation (REDD+) projects in Tanzania. Global Environmental Change, 24, 277–286. https://doi.org/10.1016/j.gloenvcha.2013.12.003

Linkie, M., Haidir, I. A., Nugroho, A., & Dinata, Y. (2008). Conserving tigers Panthera tigris in selectively logged Sumatran forests. Biological Conservation, 141(9), 2410–2415. https://doi.org/10.1016/j.biocon.2008.07.002

Losiri, C., Nagai, M., Ninsawat, S., & Shrestha, R. P. (2016). Modeling urban expansion in Bangkok metropolitan region using demographic–economic data through cellular Automata-Markov chain and multi-layer perceptron-Markov chain models. Sustainability, 8(7), 686. https://doi.org/10.3390/su8070686

Lukas, P., Melesse, A. M., & Kenea, T. T. (2023). Prediction of Future Land Use/Land Cover Changes Using a Coupled CA-ANN Model in the Upper Omo–Gibe River Basin, Ethiopia. Remote Sensing, 15(4), 1148. https://doi.org/10.3390/rs15041148

Mas, J. F., Kolb, M., Paegelow, M., Olmedo, M. T. C., & Houet, T. (2014). Inductive pattern-based land use/cover change models: A comparison of four software packages. Environmental Modelling & Software, 51, 94–111. https://doi.org/10.1016/j.envsoft.2013.09.010

Mas, J. F., Puig, H., Palacio, J. L., & Sosa-López, A. (2004). Modelling deforestation using GIS and artificial neural networks. Environmental Modelling & Software, 19(5), 461–471. https://doi.org/10.1016/S1364-8152(03)00161-0

Monteiro, A. T., Fava, F., Hiltbrunner, E., Marianna, G. D., & Bocchi S. (2011). Assessment of land cover changes and spatial drivers behind loss of permanent meadows in the lowlands of Italian Alps. Landscape and Urban Planning, 100(3), 287–294. https://doi.org/10.1016/j.landurbplan.2010.12.015

Mostafazadeh, R., & Talebi Khiavi, H. (2024). Landscape change assessment and its prediction in a mountainous gradient with diverse land-uses. Environment, Development and Sustainability, 26(2), 3911–3941. https://doi.org/10.1007/s10668-022-02862-x

Munsi, M., Areendran, G., & Joshi, P. K. (2012). Modeling spatio-temporal change patterns of forest cover: a case study from the Himalayan foothills (India). Regional Environmental Change, 12(3), 619–632. https://doi.org/10.1007/s10113-011-0272-3

Naboureh, A., Ebrahimy, H., Azadbakht, M., Bian, J., & Amani, M. (2020). RUESVMs: An ensemble method to handle the class imbalance problem in land cover mapping using Google Earth Engine. Remote Sensing, 12(21), 3484. https://doi.org/10.3390/rs12213484

Nagabhatla, N., Finlayson, C. M., Sellamuttu, S. S., & Gunawardena, A. (2008). Application of geospatial tools to monitor change in a micro-tidal estuary for the purpose of management planning. Ceylon Journal of Science (Biological Sciences), 37(1), 73–86. https://doi.org/10.4038/cjsbs.v37i1.497

Nehzak, H. K., Aghaei, M., Mostafazadeh, R., & Rabiei-Dastjerdi, H. (2022). Assessment of machine learning algorithms in land use classification. In Computers in Earth and Environmental Sciences (pp. 97–104). Elsevier. https://doi.org/10.1016/B978-0-323-89861-4.00022-1

Nyatuame, M., Agodzo, S., Amekudzi, L. K., & Mensah-Brako, B. (2023). Assessment of past and future land use/cover change over Tordzie watershed in Ghana. Frontiers in Environmental Science, 11, 1139264. https://doi.org/10.3389/fenvs.2023.1139264

Ozturk, D. (2015). Urban growth simulation of Atakum (Samsun, Turkey) using cellular Automata-Markov chain and multi-layer Perceptron-Markov chain models. Remote Sensing, 7(5), 5918–5950. https://doi.org/10.3390/rs70505918

Rafiee, R., Mahiny, A. S., Khorasani, N., Darvishsefat, A. A., & Danekar, A. (2009). Simulating urban growth in Mashad City, Iran through the SLEUTH model (UGM). Cities, 26(1), 19–26. https://doi.org/10.1016/j.cities.2008.11.005

Rozenstein, O., & Karnieli, A. (2011). Comparison of methods for land-use classification incorporating remote sensing and GIS inputs. Applied Geography, 31(2), 533–544. https://doi.org/10.1016/j.apgeog.2010.11.006

Saadat, H., Adamowski, J., Bonnell, R., Sharifi, F., Namdar, M., & Ale-Ebrahim, S. (2011). Land use and land cover classification over a large area in Iran based on single date analysis of satellite imagery. ISPRS Journal of Photogrammetry and Remote Sensing, 66(5), 608–619. https://doi.org/10.1016/j.isprsjprs.2011.04.001

Saravanan, S., Jacinth, J. J., Singh, L., Saranya, T., & Sivaranjani, S. (2019). Impact of land-use change on soil erosion in the Coonoor Watershed, Nilgiris Mountain Range, Tamil Nadu, India. In Advances in Remote Sensing and Geo Informatics Applications (pp. 109–111), Springer. https://doi.org/10.1007/978-3-030-01440-7_26

Sarif, M. O., & Gupta, R. D. (2022). Spatiotemporal mapping of Land Use/Land Cover dynamics using Remote Sensing and GIS approach: a case study of Prayagraj City, India (1988–2018). Environment, Development and Sustainability, 24(1), 888–920. https://doi.org/10.1007/s10668-021-01475-0

Schneider, S. C., Biberdžić, V., Braho, V., Gjoreska, B. B., Cara, M., Dana, Z., ... & Vermaat, J. E. (2020). Littoral eutrophication indicators are more closely related to nearshore land use than to water nutrient concentrations: A critical evaluation of stressor-response relationships. Science of the Total Environment, 748, 141193. https://doi.org/10.1016/j.scitotenv.2020.141193

Schulz, J. J., Cayuela, L., Rey-Benayas, J., M., & Schröder, B. (2011). Factors influencing vegetation cover change in Mediterranean Central Chile (1975–2008). Applied Vegetation Science, 14(4), 571–582. https://doi.org/10.1111/j.1654-109X.2011.01135.x

Shao, Y., & Lunetta, R. S. (2012). Comparison of support vector machine, neural network, and CART algorithms for the land-cover classification using limited training data points. ISPRS Journal of Photogrammetry and Remote Sensing, 70, 78–87. https://doi.org/10.1016/j.isprsjprs.2012.04.001

Singh, S. K., Laari, P. B., Mustak, S. K., Srivastava, P. K., & Szabó, S. (2018). Modelling of land use land cover change using earth observation data-sets of Tons River Basin, Madhya Pradesh, India. Geocarto International, 33(11), 1202–1222. https://doi.org/10.1080/10106049.2017.1343390

Singh, V. G., Singh, S. K., Kumar, N., & Singh, R. P. (2022). Simulation of land use/land cover change at a basin scale using satellite data and markov chain model. Geocarto International, 37(26), 11339–11364. https://doi.org/10.1080/10106049.2022.2052976

Talebi Khiavi, H., & Mostafazadeh, R. (2021). Land use change dynamics assessment in the Khiavchai region, the hillside of Sabalan mountainous area. Arabian Journal of Geosciences, 14, 2257. https://doi.org/10.1007/s12517-021-08690-z

Talebi Khiavi, H., Mostafazadeh, R., Asaadi, M. A., & Namini. S. K. A. (2022). Temporal land use change and its economic values under competing driving forces in a diverse land use configuration. Arabian Journal of Geosciences, 15, 1597. https://doi.org/10.1007/s12517-022-10890-0

Thanh Noi, P., & Kappas, M. (2018). Comparison of random forest, k-nearest neighbor, and support vector machine classifiers for land cover classification using Sentinel-2 imagery. Sensors, 18(1), 18. https://doi.org/10.3390/s18010018

Thiha, S., Shamseldin, A. Y., & Melville, B. W. (2021). Assessment of the Myitnge River flow responses in Myanmar under changes in land use and climate. Modeling Earth Systems and Environment, 7(3), 1393–1415. https://doi.org/10.1007/s40808-022-01458-8

Ullah, M., Li, J., & Wadood, B. (2020). Analysis of urban expansion and its impacts on Land surface temperature and vegetation using RS and GIS, A case study in Xi'an City, China. Earth Systems and Environment, 4(3), 583–597. https://doi.org/10.1007/s41748-020-00166-6

Václavík, T., & Rogan, J. (2009). Identifying trends in land use/land cover changes in the context of post-socialist transformation in Central Europe: A case study of the greater Olomouc region, Czech Republic. GIScience & Remote Sensing, 46(1), 54–76. https://doi.org/10.2747/1548-1603.46.1.54

Verburg, P. H., Kok, K., Pontius, R. G., & Veldkamp, A. (2006). Modeling land-use and land-cover change. In Land-use and land-cover change (pp. 117–135). Springer. https://doi.org/10.1007/3-540-32202-7_5

Verburg, P. H., Soepboer, W., Veldkamp, A., Limpiada, R., Espaldon, V., & Mastura, S. S. A. (2002). Modeling the Spatial Dynamics of Regional Land Use: The CLUE-S Model. Environmental Management, 30(3), 391–405. https://doi.org/10.1007/s00267-002-2630-x

Wang, J., Yin, X., Liu, S., & Wang, D. (2023). Spatiotemporal change and prediction of land use in Manasi region based on deep learning. Environmental Science and Pollution Research, 30(34), 82780–82794. https://doi.org/10.1007/s11356-023-27826-0

Yang, R., Zhang, J., Xu, Q., & Luo, X. (2020). Urban-rural spatial transformation process and influences from the perspective of land use: A case study of the Pearl River Delta Region. Habitat International, 104, 102234. https://doi.org/10.1016/j.habitatint.2020.102234

Zabihi, M., Moradi, H., Gholamalifard, M., Khaledi Darvishan, A., & Fürst, C. (2020). Landscape Management through Change Processes Monitoring in Iran. Sustainability, 12(5), 1753. https://doi.org/10.3390/su12051753

Zhan, C., & Xie, M. (2022). Land use and anthropogenic heat modulate ozone by meteorology: a perspective from the Yangtze River Delta region. Atmospheric Chemistry and Physics, 22(2), 1351–1371. https://doi.org/10.5194/acp-22-1351-2022

Article first received: 11 December 2024
Article accepted: 13 August 2025